Investigating failure in flax-polypropylene natural composites using discrete textile models and continuum damage mechanics approach

S. M. Panamoottil[a], R. Das[b] and K. Jayaraman[c]

Centre for Advanced Composite Materials, Department of Mechanical Engineering, University of Auckland, Auckland 1010, New Zealand

[a]span082@aucklanduni.ac.nz, [b]r.das@auckland.ac.nz, [c]k.jayaraman@auckland.ac.nz

Keywords: Natural fibre composites; failure criteria; fracture mechanics; damage model; Finite Element Method.

Abstract. Natural fibre composites (NFCs) are currently applied primarily in secondary structural or non-load-bearing applications, such as in the door panels and underbodies of automobiles. However, improvements in processing and treatment methods for natural fibres point towards their future application to primary structural components. In this context, their fracture and progressive damage behaviour become important, and this paper aims to assess the applicability of anisotropic continuum damage modes to evaluate their failure behaviour under quasi-static tensile loading. The damage approach was applied to composites of polypropylene with unidirectional (UD) and woven flax fabric composites. Elastic properties, strength limits, and notched strengths were obtained for the composites, and notched strengths modelled analytically using the modified point stress criterion. Subsequently, the validity of a continuum damage model for predicting failure modes of NFCs was examined. Simulations were performed on a 0.22 volume fraction UD composite, and a 0.19 volume fraction woven composite. Predictions for notched strengths using the analytical models were good for the smaller radii, but under-predicted strengths for the largest radius, which could be due to the different failure behaviours of NFCs. Results from the damage simulations showed good agreement between the simulated and experimental loading curves for the initial portion of the loading curves. The results show that damage models could potentially be used for more accurate predictions of failure behaviour of natural fibre composites, aiding the design of high strength and fracture resistant structures incorporating such materials.

Introduction

Composites are a group of materials which demonstrate very high specific properties, and have been applied to several areas where a light-weight design without degradation in performance is required. For the analysis of composite structures, failure loads have been typically determined using relatively expensive physical testing or via numerical methods. While numerical methods definitely possess the advantage of economy, these models have to describe material behavior in a manner similar to that encountered in physical reality. In this context, current numerical models take advantage of the fact that composites possess significant load carrying capacity beyond the first failure initiation point. Such behavior is typically incorporated using one or more of the commonly used composite failure criteria [1] combined with material degradation models [2]. As reviewed by Garnich and Akula [2], several degradation models exist, ranging from sudden degradation to thermodynamically-based damage mechanics methods. Current failure theories, along with a progressive damage analysis, are reasonably equipped to predict composite failures in that they take account of the fact that even though failure might have initiated at some parts of the composite, it can still strain to some extent before final failure. With a proper choice of degradation damage

factors, such models can predict failure limits close to actual values. The accuracy of such predictions provides designers the option to choose lower factor of safety values, resulting in lighter and more efficient structures.

In the backdrop of dwindling mineral resources and a global call for recovery and recyclability of materials, composite manufacturers need to reduce the environmental impact of their products while maintaining performance at acceptable levels. Natural fibre composites (NFCs) can help in the reduction of the environmental footprints of composite products, while progressive damage analysis as described above can help in exploiting the post-failure strain of natural fibre composites and prolonging their usage.

There have been several attempts to analyse the properties of NFCs experimentally. However, theoretical or numerical analyses of their behaviour have been limited to semi-empirical approaches, such as the point stress criterion (PSC) [3], and cohesive zone models for fibre-matrix interface [4] and inter-fibre lamellae in flax fibres [5]. To the knowledge of the authors, there have been no studies yet which have utilized a progressive damage approach to model the meso-scale behavior of natural composites, and hence, the applicability of such models to NFCs will be investigated. This study will experimentally determine the elastic properties and strength limits of fabric composites. Discrete finite element models of the fabric composites will be produced, incorporating anisotropic damage behaviour with progressive failure. The different failure modes of natural fibre composites will be considered and the interactions between them taken into account by use of suitable degradation factors in the damage model. The results from the numerical models will be compared to experimental behaviour for tensile test geometries.

Methodology

Materials. Polypropylene (PP) of grade Moplen RP241G was supplied by Field International Ltd., and flax fabrics of codes C003 (unidirectional stitched) and C008 (balanced twill weave) were supplied by Libeco NV, Belgium. Details of the fabrics are given in Table 1. PP sheets of two thicknesses, 0.38 mm and 0.6 mm, were used in the manufacture.

Table 1. Properties of flax fabrics used in study

Fabric designation	Warp		Weft		Areal density [g/m^2]	Weave
	Threads/ cm	Yarn Density [Tex]	Threads/cm	Yarn Density [Tex]		
FLAXDRY C003	42.5	41.7	3	27.8	190	Ribs 4/4 – UD
FLAXDRY C008	25.1	27.8	24	27.8	150	Twill 2/2

Composite and specimen fabrication. Composites laminates of 3 mm thickness were prepared by compression moulding, stacking layers of polymer sheets and flax fabric in a symmetrical manner, with thin Teflon sheets on the top and bottom ends of the stack. All the materials were dried for 10 hours at 80˚C before processing, and proportions were measured based on weight and later converted into volume fractions using the appropriate densities. The die used for compression moulding was a matched male-female combination forming a square cavity, with metal inserts which can be used to vary the composite thickness required for one particular cycle. The die was heated to 190˚C, after which the assembly of polymer sheets and flax fabric was inserted into the die, after which a pressure of 0.5 MPa was applied, maintaining the die temperature at 190˚C for 10 minutes. Subsequently, the pressure was increased to 6.5 MPa, and the dies were then cooled

holding the pressure. For laminates A and C (in Table 2), 0.38 mm PP sheets were used, whereas for laminates B and D, 0.6 mm PP sheets were used.

Table 2. Composite panels produced and designations. In the layup column, 'P' refers to a layer of polypropylene, and 'F' refers to a layer of flax fabric.

Laminate designation	Matrix	Fabric	Fibre volume fraction Vf	Layup
A	PP RP241G	FLAXDRY C003	0.22	PFPFPFPFPFP
B	PP RP241G	FLAXDRY C003	0.41	PFFFFFPFFFFFP
C	PP RP241G	FLAXDRY C008	0.19	PFPFPFPFPFPFP
D	PP RP241G	FLAXDRY C008	0.41	PFFFFFFPFFFFFFP

Testing. Tensile, in-plane shear and compressive specimens, in the geometries specified by the ASTM D3039, ASTM D4255 and ASTM D6641, respectively, were cut from the panels manufacture, using a laser cutter. The properties in both longitudinal and transverse directions were tested using an Instron 5567 UTS. Eight specimens each were tested during each tensile test at a crosshead speed of 2 mm/min. Eight specimens were also tested during each compressive test, for which the crosshead speed used was 1.3 mm/min. Five specimens each were tested for shear properties, at a crosshead speed of 1.5 mm/min.

Some of the tensile test specimens were used for notched strength tests. Circular holes were introduced at the centre of these specimens using an end mill, and good finish was ensured by clamping the specimen between two sacrificial layers of similar composite material before milling. For each material system, three hole sizes (3, 6 and 10 mm), and three specimens for each of the hole sizes were tested.

Analytical notched strength. Notched strengths obtained from the tensile tests of notched specimens were used to calculate the characteristic distance value for each material system, using the point stress criterion [6]. However, when the average value of characteristic distance from the specimens with the three different hole sizes were used for notched strength prediction, the predicted values were 20 - 40% different from the experimental values. Hence, it is clear that characteristic distance is not a material system constant, and so the modified point stress criterion (PWG) [7] was used to model characteristic distance as a function of notch radius, as given in the equation below:

$$d_0 = \frac{1}{c}\left(\frac{R}{R_0}\right)^m \tag{1}$$

where R_0 is the reference radius, set to half of width in this case, c is the notch sensitivity factor, and m is the exponential factor. c and m are curve fitting parameters, and were calculated from the experimental notched strength results.

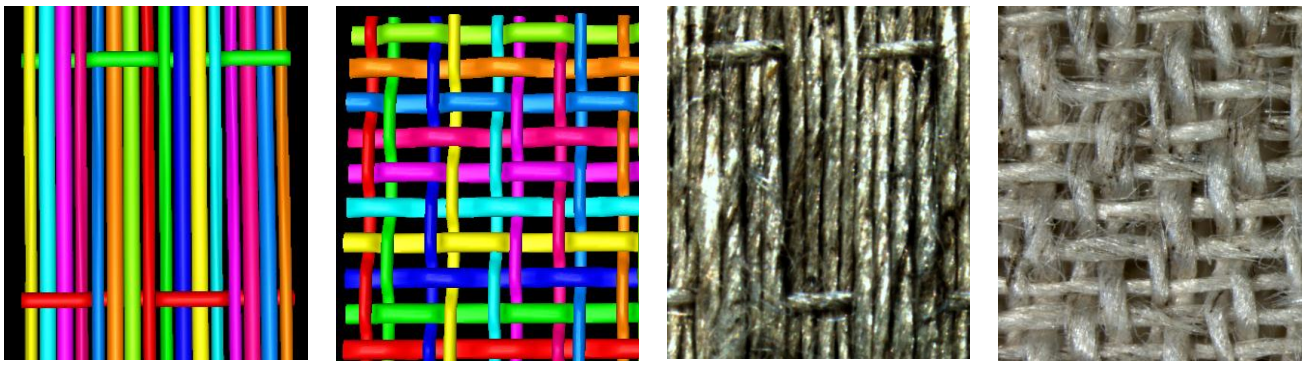

(a) (b) (c) (d)

Fig. 1. Models of flax fabrics generated by Texgen: a,b- Models for FLAXDRY C003, and FLAXDRY C008; c,d – actual fabric images for C003 and C008 respectively.

The elastic properties of the matrix-impregnated yarn elements were calculated using RoM for longitudinal properties and modified Halpin-Tsai equations [8] for transverse properties, using a maximum packing fraction of 0.907 (hexagonal packing). In order to obtain yarn volume fractions, sections were made from panels of the composite for each material system and for each volume fraction. After polishing, optical analysis of area fractions of the yarns in several sections yielded the apparent volume fraction of yarns in the composite for each configuration. Due to resin impregnation of the yarns, they are expected to occupy more volume in the composites than the volume they should occupy based on the actual fibre volume fraction calculated using density of the composites. The amount of matrix present in the yarns can be calculated from actual and apparent volume fractions, and from this the proportion of matrix in the resin-impregnated yarns can be determined.

Optical measurements. Various optical measurements, such as the centre-to-centre distance between individual warp yarns and individual weft yarns, were performed on the fabrics used so as to obtain parameters required for the modelling of the yarn paths, crossovers and spacings, which constitute the architecture of the fabric. The discrete composite models, including yarn geometry and matrix, were generated in Texgen (shown in Fig. 1).
Optical measurements were also performed on polished cross-sections of the composites to determine the area fraction of fibres in them. Images for optical measurements (including textile geometry) were captured using a Leica MZ16 microscope.

Numerical Modelling. For the numerical modeling, an approach similar to that followed by Gan *et. al.* [9] was adopted. Finite element models representative of half the gauge section of the tensile test specimens, with matrix and fabric yarns modeled separately, were generated using the Python interface of Texgen software [10]. Discrete modelling of textiles enables simulation incorporating the interaction between warp and weft yarns, and also allows modelling of the failure of the yarns individually and distinctly from that of the matrix.
Half models of the 50 · 25 mm^2 gauge sections were used to reduce computational time because of the large number of yarns present per unit length, and numerical simulations were performed for composites A and C (unidirectional vf 0.22 and woven vf 0.22 in Table 2). The discrete composite models were exported to an ABAQUS input file using the voxel mesh output option in Texgen. These files were then modified to include material properties, boundary conditions, element sets and other control parameters required for analysis. The yarn elements were assigned the transversely isotropic properties determined earlier, and the matrix elements were assigned their isotropic

properties. Voxel sizes were chosen for each composite model such that each yarn was continuous without overlapping with other yarns, and the resulting sizes chosen were: Composite A – 0.135 0.163 0.085 mm^3, Composite B – 0.08 0.081 0.048 mm^3.

Table 3. Material degradation factors used in the damage model for different failure modes, as defined in the UMAT implementation. 1 – parallel to loading direction, 2 – perpendicular to loading direction, 3 – out of plane.

Failure Index i	Failure mode	Degradation factors for engineering properties					
		E_{11}	E_{22}	E_{33}	G_{12}	G_{13}	G_{23}
1	1T	0.001	0.05	0.05	0.05	0.05	0.05
2	1C	0.001	0.05	0.05	0.05	0.05	0.05
3	2T	1	0.001	0.05	0.2	0.2	0.2
4	2C	1	0.001	0.05	0.2	0.2	0.2
5	3T	1	0.05	0.001	0.2	0.2	0.2
6	3C	1	0.05	0.001	0.2	0.2	0.2
7	12	1	0.05	0.05	0.05	0.05	1
8	13	1	0.05	0.05	1	1	0.05
9	23	1	0.05	0.05	0.05	0.05	0.05

A material damage (degradation) model was implemented in ABAQUS using the user defined material (UMAT) option. The maximum stress criteria was used to determine the onset of failure, and a sudden damage approach was used to degrade the material properties. For any material point and each of the six stress components, upon satisfying criteria for failure, the corresponding material stiffnesses were reduced by the appropriate degradation factors, listed in
Table 3.
In the failure mode column, the numbers 1, 2 and 3 represent the longitudinal, in-plane transverse and out-of-plane transverse directions, respectively. The letters ‘T’ and ‘C’ represent failure by tension and compression, respectively, and 12, 13 and 23 represent shear failure in the corresponding planes.
For the numerical simulations, the gauge section was fully fixed at the bottom end, and the top end was displaced at the same rate used during the physical tensile tests. Also, since a half model was used, symmetry conditions were imposed along the plane of symmetry.
Strain values parallel to the loading direction (longitudinal direction) were obtained from two points lying on the same line along the length of the model, and separated by 25 mm, similar to the method employed during experiments. For a set of elements located at the middle of the specimen, longitudinal stresses were obtained and averaged. Plots of stress-strain data were then generated to compare results obtained from the model to the experimental data from the tensile tests.

Results and Discussion

Analytical notched strength predictions. In Fig. 2, the first letter in the legend refers to the corresponding laminate from Table 2. The points represent experimental data, and the lines are fitted to the points using curve fitting, as suggested in the modified point stress criterion approach. The characteristic distance fits are quite good for A and B (UD composites); however, there is a large difference in the case of C and D (woven composites), and especially so for D. However, when it comes to notched strength predictions, good fit was obtained for only B, with predicted values for A being nearly 10% different from the experimental values, and those for both C and D under-predicting the notched strength by nearly 30% for notch radius of 10 mm. The predictions do not

match very well for the larger notch radius of 10 mm. The failure behaviour of natural fibre composites vary from those of synthetic ones due to inter-fibre shear failure. This behaviour might be dominant at larger notch radii.

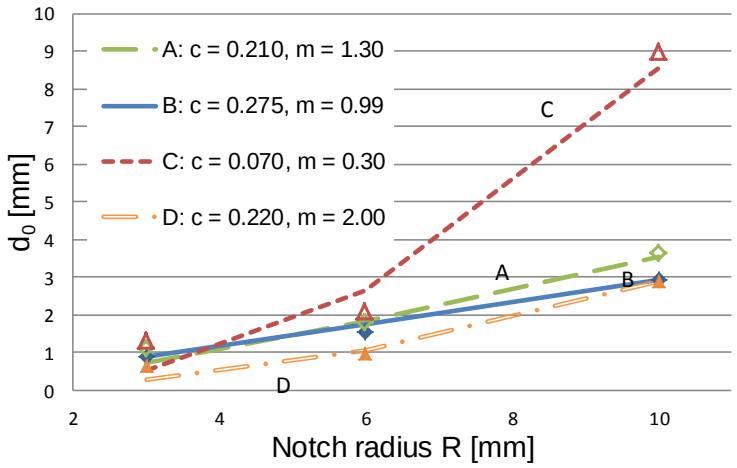

Fig. 2. Characteristic distance values for unidirectional (A, B) and woven (C, D) composites for notch radii of 3, 6 and 10 mm.

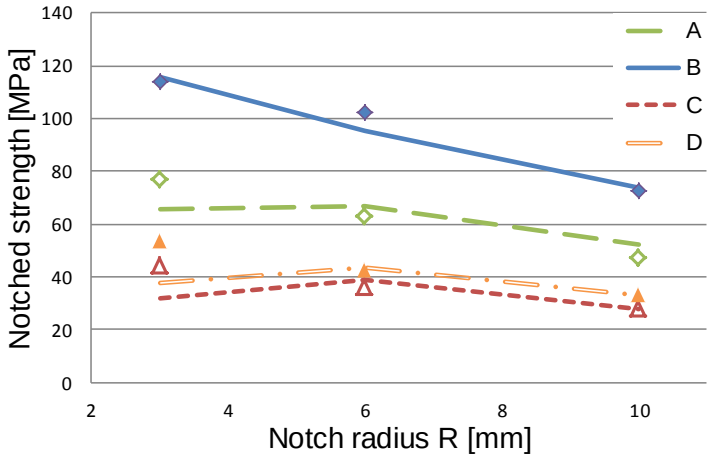

Fig. 3. Notched strength predictions vs. experimental results for the unidirectional (A, B) and woven (C, D) composites, with notch radii of 3, 6 and 10 mm.

Elastic properties. Listed in Numerical results**.** The results of numerical simulations performed on the half symmetry models generated for composites A and C (see Table 2) are shown below (Fig. 4). For fabric composites, due to the presence of yarns along both directions, at a certain stage of the tensile deformation process, the initial linear stiffness reduces due to failure of the weft yarns. This is taken into account in the damage model by assigning appropriate degradation factors (Table 3) to reduce the transverse stiffness of the yarns for the corresponding transverse direction, once the strength limit in that direction is exceeded.

Table 4 are the theoretical elastic properties of flax fibre and the experimentally determined properties for the polypropylene matrix. Here X_T, Y_T and Z_T represent tensile strengths in the X, Y and Z directions, respectively, and X_C, Y_C and Z_C represent compressive strengths in the X, Y and Z

directions, respectively. S_{12}, S_{13}, and S_{23} represent shear strengths in the 12 (XY), 13 (XZ) and 23 (YZ) planes, respectively.

Numerical results. The results of numerical simulations performed on the half symmetry models generated for composites A and C (see Table 2) are shown below (Fig. 4). For fabric composites, due to the presence of yarns along both directions, at a certain stage of the tensile deformation process, the initial linear stiffness reduces due to failure of the weft yarns. This is taken into account in the damage model by assigning appropriate degradation factors (
Table 3) to reduce the transverse stiffness of the yarns for the corresponding transverse direction, once the strength limit in that direction is exceeded.

Table 4. Elastic modulii and strengths of flax fibre and polypropylene.

Property	**Flax fibre**	**Polypropylene**
E_{11} [GPa]	46.45	0.899
$E_{22} = E_{33}$ [GPa]	2.5	
v_{12}	0.3	0.3
v_{23}	0.3	
G_{12} [GPa]	3.72	0.69
G_{23} [GPa]	6.88	
X_T [MPa]	450	22
X_C [MPa]	50	46
$Y_T = Z_T$ [MPa]	5	22
$Y_C = Z_C$ [MPa]	8	46
$S_{12} = S_{13}$ [MPa]	0	39
S_{23} [MPa]	75	39

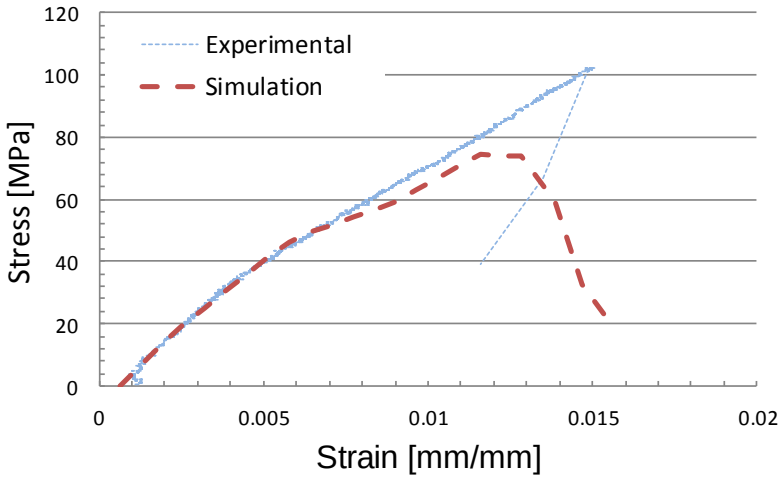

(a)

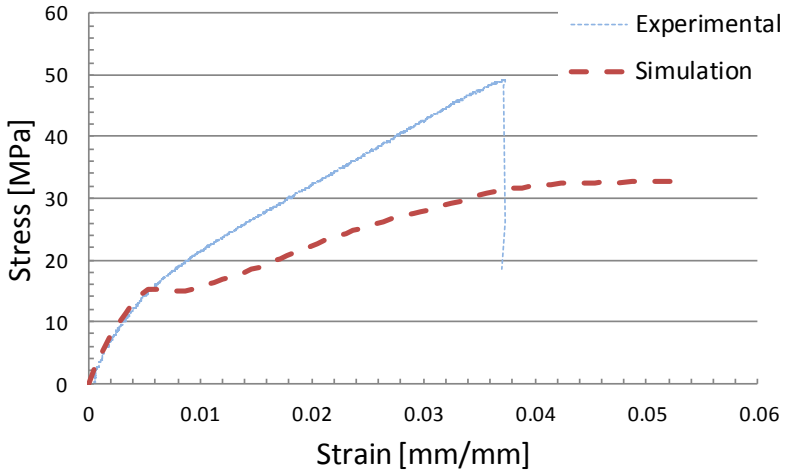

(b)

Fig. 4. Comparison of tensile stress-strain plots between experimental results and numerical simulations for (a) composite A (0.22 volume fraction unidirectional fabric composite), and (b) composite B (0.19 volume fraction woven fabric composite).

The simulated stress-strain curves of both composites match the corresponding experimental results up to strains of approximately 0.6%, after which a deviation is observed (Fig. 4). However, the ultimate strengths were under-predicted by 25% for the unidirectional composite and by nearly 40% for the woven composite. The low strength predictions may be attributed to several factors, such as mesh density used per yarn and interlocking between neighbouring fibres in a given matrix impregnated yarn. Mesh density was limited due the large number of yarns present in the gauge region, and if the numerical model of this region were to be generated with a finer mesh, the computational solution time would be expected to increase significantly.

Conclusions

The utilities of continuum damage models to simulate quasi-static damage in natural fibre Polypropylene-flax composites have been evaluated. Notched strengths of composites have been modelled semi-empirically using the modified point stress criterion. The predictions from the model agreed reasonably well with the experimental data. From damage simulations, good agreement was obtained between the experimental and numerically predicted loading curves up to strains of 0.6% for both the unidirectional and woven fabric composites. However, the strength predictions for both cases were lower than the experimentally determined values. This could be caused by the choice of FE mesh density or uncertainties in the strength limits used as inputs to the damage models. Discrete models with finer mesh will be used in future to study the effect on strength predictions. Experimental investigations on single yarns with different levels of matrix impregnation will also be attempted for direct determination of strength limits. Once accurate values for yarn strengths is achieved, these strengths will be applied to similar discrete models.

Acknowledgements

This project is funded by the Ministry of Science and Innovation Project No. 3625485. The authors would like to thank Ming Gan of the University of Auckland for assistance with the damage model implementation in ABAQUS.

References

[1] A.C. Orifici, I. Herszberg, and R.S. Thomson, Composite Structures, Vol. 86 (2008), p. 194-210
[2] M.R. Garnich and V.M.K. Akula, Applied Mechanics Reviews, Vol. 62 (2009), p. 010801-33
[3] K.S. Ahmed, S. Vijayarangan, and A.C.B. Naidu, Materials & Design, Vol. 28 (2007), p. 2287-2294
[4] M. Hbib, et al., Composites Science and Technology, Vol. 71 (2011), p. 1419-1426
[5] K. Charlet and A. Béakou, Procedia Engineering, Vol. 10 (2011), p. 906-911
[6] J.M. Whitney and R.J. Nuismer, Journal of Composite Materials, Vol. 8 (1974), p. 253-265
[7] R.B. Pipes, R.C. Wetherhold, and J.W. Gillespie, Journal of Composite Materials, Vol. 13 (1979), p. 148-160
[8] R.F. Landel and L.E. Nielsen; *Mechanical properties of polymers and composites* (Marcel Decker, New York 1994).
[9] J.M. Gan, S. Bickerton and M. Battley, ICCM18, Jeju, Korea (2011)
[10] Information on http://texgen.sourceforge.net/index.php/Main_Page